Modelling of electrosorption of ions in a flow cell

A thesis submitted towards partial fulfilment of BS-MS Dual Degree Programme

by
Aerpula Naveen

under the guidance of

Dr. R Venkataraghavan, PhD
Discover Category Leader, Water
Unilever R&D, Bangalore

Indian Institute of Science Education and Research (IISER), Pune

Certificate

This is to certify that this thesis entitled **“Modelling of electrosorption of ions in a flow cell”** submitted towards the partial fulfilment of the BS-MS dual degree programme at the Indian institute of Science Education and Research (IISER), Pune represents original research carried out by Aerpula Naveen at Unilever R&D, Bangalore, under the supervision of Dr. R Venkataraghavan during the academic year 2013-2014.

Aerpula Naveen

Dr. R Venkataraghavan

Acknowledgements

I would like to offer my profoundest gratitude to my thesis supervisor Dr. R Venkataraghavan. From helping me understanding the basics of electrosorption to the process of writing the thesis, Dr. R Venkataraghavan has offered his unreserved help and guidance. It would have been impossible to achieve this goal without his constant support and encouragement. I consider myself to be fortunate to be associated with him who has given a decisive turn to my career.

I would also like to thank Mr. Tinto J Alencherry, who was involved in this project from the start and was a great help in completing my thesis. His support and positive inputs have been invaluable.

Table of Contents

List of Figures

List of Tables

Abstract

Salt removal through electrosorption is an electric field mediated adsorption phenomena that is based on the applied potential, nature and area of the electrode surface and concentration of salt in the electrolyte. Understanding of the phenomena can help establish the limits of adsorption (salt removal), the kinetics and its efficiency. In this thesis, we investigate the change in the effluent salt concentration with time and its dependence on operation parameters, through modelling a electrosorption process in a flow cell. We model the salt removal and electrosorption kinetics, using the Gouy-Chapman-Stern (GCS) layer model and a modified donnan (mD) model, with applied potential, flow rate in simple electrode cell. The proposed models were solved using finite element based simulation package (COMSOL). It is seen that the results compare favourably with experimental data (provided by Unilever) for the change of the effluent salt concentration in time.

1 Introduction

The availability of affordable clean water is one of the key social, economic and technological challenges of the 21st century. Since, fresh water is limited, an alternate approach is to deionize/desalinate brackish or sea water. Over the years a number of deionization methods have been developed, among which multi-stage flash distillation and reverse osmosis are now the most commonly known and wide spread technologies. Multi-stage flash distillation and reverse osmosis are energy intensive. However, a more recent technology, Capacitive deionization (CDI), has shown promise to make deionisation energy efficient and affordable. CDI works on the principle of electrosorption of ions on a charged substrate (electrode). Electrosorption is a fundamental mechanism by which ions adsorb on a charged electrode under the influence of an electric field from the electrolyte solution. It is therefore important to understand the principles governing electrosorption to exploit this technology, and this is attempted in our work.

Several publications are available to provide a basic understanding of the fundamental physics behind electrosorption process. General models of electrosorption process commonly focus on the interactions between the electrode and the solution within the pores of the electrode. There are many theories available to describe these interactions, among them Poisson-Nernst-Plank (PNP) equations [1], capacitive adsorption of ions at the electrode-electrolyte interface [2, 3] and the electrical double layer structure on the ionic adsorption [4, 5] are important. Electrosorption phenomena are however best described by electrical double layer theories and modelled by two double layer models namely the Gouy-Chapman-Stern (GCS) layer model and modified Donnan (mD) model to describe electrosorption phenomena. Earlier, we attempted to model the phenomena using a Langmuir type adsorption, together with Poisson-Nernst-Plank (PNP) equations, which is described in Appendix B.

Analyzing the electrosorption process by using modelling method is important, since it can provide a detailed understanding of electrosorption in the flow cell. As a result, the mechanism of the ion adsorption can be described and the performance of the electrosorption under different operational conditions can be predicted. We

use COMSOL Multi-physics software package to model the electrosorption phenomenon. It is a finite element method based, solver and simulation software package for various physics and engineering applications, especially coupled phenomena or multiphysics. It allows for entering coupled systems of partial differential equation (PDEs). The PDEs can be entered directly by using equation based physics interface. It has a strong geometrical interface to import/represent complicated shapes and features in which the solution for the relevant physics based simulation is required.

Electrosorption experiments were performed by using an electrode flow cell (Fig. 1). As shown in Figure 1.1, an electrical potential difference (also called as cell voltage, V_{cell}) was applied between the two oppositely placed porous carbon electrodes. Because of the cell voltage, ions from the feed solution become immobilized by electrosorption process and are removed and stored inside the pores within the electrodes, where electrostatic double layers (EDL) are formed. As a result cations are stored in the cathode (the electrode into which negative electrical charge is transferred) and anions in the anode (the electrode into which positive electrical charge is transferred), thereby partially deionising the feed water (fresh water). There are two ways to perform these electrosorption experiments: (1) batch-mode (BM), see Figure 2 a, and (2) single-pass mode (SPM), see Figure 2 b. In the batch mode, a fixed volume of water in a storage vessel was passed through the flow cell at a given flow rate and returned to the same storage vessel. The conductivity, σ, of the water (salt concentration) was constantly monitored throughout the experiment. In SPM, water was fed from a storage vessel and the conductivity, σ, of the water leaving the flow cell was constantly monitored. These experiments were performed separately (performed by Unilever) and the data was made available for the purpose of validation of the theoretical work presented here.

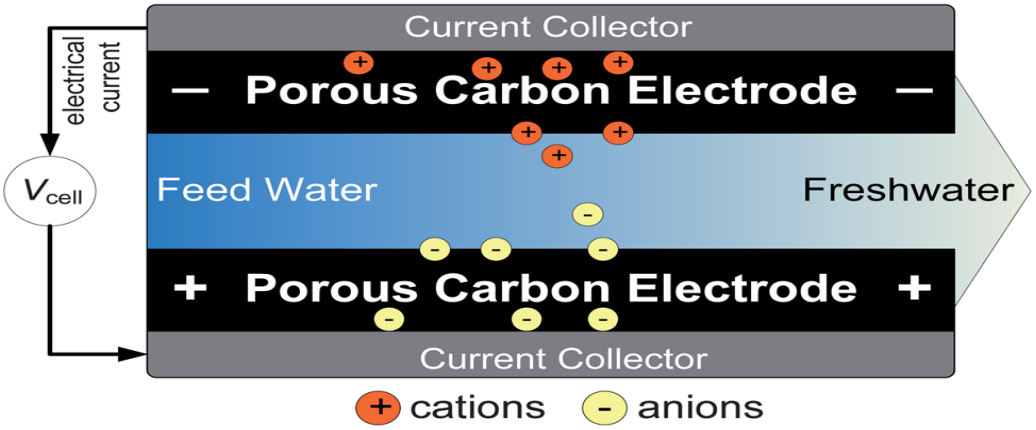

Fig. 1: Schematic representation of Electrosorption cell [6].

In this project, we aim to model the electrosorption phenomena in a flow cell by understanding the ion adsorption at the electrode interface and compare the results of the model to adsorption experiments and predict role of operational parameters and their influence on deionization process.

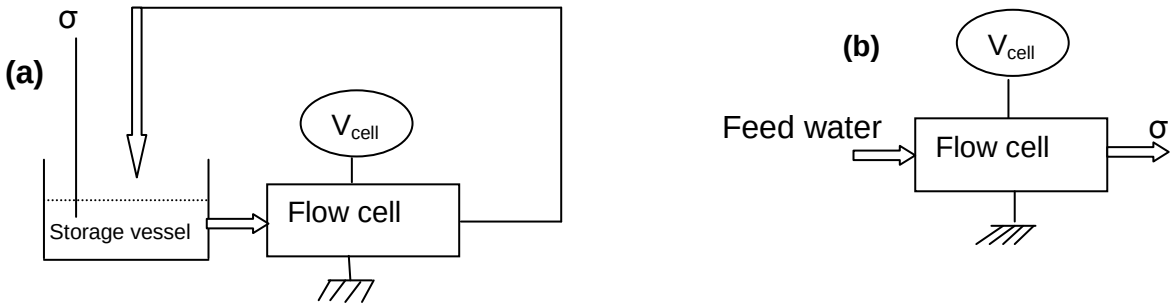

Fig. 2: Schematic representation of electrosorption experiments, (a) batch-mode experiments, (b) single-pass mode experiments.

2 Theory for Ion Transport and Electrosorption

2.1 Electrostatic Double Layer Models

The double layer models are used to visualize the ionic environment and charge storage in the vicinity of a charged surface. When most surfaces placed in contact with an electrolyte solution, surfaces acquires surface charge. This surface charge can be attributed to a variety of phenomenon but most commonly charge storage and specific adsorption of ions. The surface charge will affect the distribution of ions within close vicinity of interface (electrode/electrolyte interface). Counter-ions

of opposite charge to the surface will be attracted, while co-ions will be affected by repulsive Coulomb force. The resulting distribution of ions near the electrode surface is distinct from the electro- neutrality prescribed in bulk and is termed the electric double layer (EDL). A large number of models are available to describe the structure of the EDL at planar surfaces and in the pores of electrodes. Among them Helmholtz model, Gouy-Chapman (GC), Gouy-Chapman-Stern (GCS) model and modified donnan (mD) model are well-known models to describe the structure of EDLs.

Key property of the porous electrodes is the charge efficiency **Λ** of the electrical double layer which describes the how many ions are removed from the solution that is transferred from one electrode to the other.

2.1.1 Helmholtz Double Layer Model

Helmholtz [7], who was the first to think about charge separation at interfaces, proposed that the counter-charge in solution also resides at the surface. In other words, all the surface charge is directly neutralized by opposite sign counter ions adsorbed to the surface, see Figure 3 a. The interactions between the ions in solution and the electrode surface were assumed to be electrostatic in nature and resulted from the fact that electrode holds a charge density, σ, which arises from either an excess or deficiency of electrons at the electrode surface. The locus of centres of these ions which are having opposite polarity to the surface is called the outer Helmholtz plane (OHP). Such a structure is equivalent to a parallel-plate capacitor, which has the following relation between the stored charge density, σ, and the voltage drop, ψ, between the plates:

$$\sigma = \frac{\varepsilon_0 \varepsilon_r}{d} \psi \qquad (2.1.1.1)$$

Where ε_0 is the permittivity of free space ε_r is the relative permittivity of the medium and d is the interplate spacing. The double layer differential capacitance of the Helmholtz layer is therefore

$$\frac{\partial \sigma}{\partial \psi} = C_H = \frac{\varepsilon_0 \varepsilon_r}{d} \qquad (2.1.1.2)$$

The weakness of this model is immediately apparent in Eq. 2.1.1.2, which predicts that C_H is a constant i.e., this model does not account for the dependence of the capacitance on potential and electrolyte concentration. Another drawback is the neglect of interactions that occur away from the OHP. Because of these drawbacks, Helmholtz-model does not adequately explain the all the features of the EDL structure in carbon electrodes.

Instead, we must consider that ions do not condense in a plane right next to the surface, but remain diffusively distributed in a layer close to the surface as described by Gouy-Chapman.

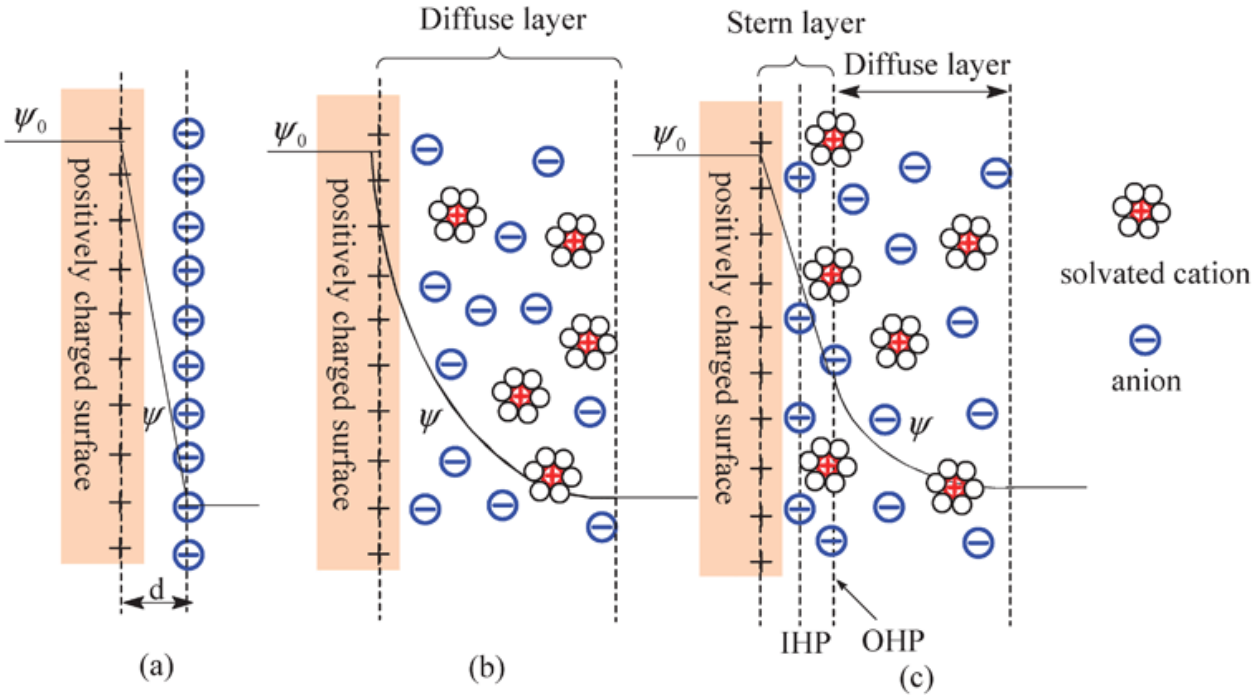

Fig. 3: Schematic representation of the electrical double layer models [8]: (a) the Helmholtz model, (b) the Gouy-Chapaman model, and (c) the Gouy-Chapman-stern layer model

2.1.2 Gouy-Chapman (GC) Double Layer Model

Gouy and Chapman [9, 10] were the first to consider the thermal motion of ions in the electrolyte solutions, which are driven by the coupled influences of diffusion and electrostatic forces. Even though the charge on the electrode is confined to the surface, the same is not necessarily true of the solution. Thus electrolyte concentrations have a phase with a relatively low density of charge

carriers, see Figure 3 b. It may take some significant thickness of solution to accumulate the excess charge needed to counterbalance surface charge. A finite thickness would arise essentially because there is interplay between the tendency of the charge on the electrode phase to attract or repel the carriers according to polarity and the tendency of thermal process to randomize them. This model therefore involves a diffuse layer of charge in the solution. There would be higher concentrations of excess charge adjacent to the electrode where electrostatic forces are most able to overcome, and lesser concentrations would be found at greater distances as those forces become weaker. Gouy and Chapman independently proposed the idea of a diffuse layer in which the concentration of the counter ions near the electrode surface follows the Boltzmann distribution.

$$c_i = c_i^0 \exp\left(\frac{-z_i e\psi}{k_B T}\right) \qquad (2.1.2.1)$$

Where ψ is measured with respect to the bulk solution, z_i is the charge on ion i, e is the electronic charge, k_B is the Boltzmann constant and T is the absolute temperature.

The total space charge density is then

$$\rho(x,y,z) = \sum_i c_i z_i e = \sum_i c_i^0 z_i e \exp\left(\frac{-z_i e\psi}{k_B T}\right) \qquad (2.1.2.2)$$

Where i runs over all ionic species. From electrostatics in 1D, we know that ρ(x) is related to the potential at distance x by the Poisson equation:

$$\frac{\partial^2 \psi}{\partial x^2} = -\frac{\rho(x)}{\varepsilon_r \varepsilon_0} \qquad (2.1.2.3)$$

Combining Eq. 2.1.2.2 and Eq. 2.1.2.3 leads to the Poisson-Boltzmann equation:

$$\frac{\partial^2 \psi}{\partial x^2} = -\frac{e}{\varepsilon_r \varepsilon_0} \sum_i c_i^0 z_i \exp\left(\frac{-z_i e\psi}{k_B T}\right) \qquad (2.1.2.4)$$

For the following boundary conditions

$x=0 \quad \psi=\psi_0$

$x=\infty \quad \psi \to 0 \quad \left(\frac{\partial \psi}{\partial x}\right) = 0$ (2.1.2.5)

Where ψ_0 is the potential at the electrode surface. Solving Eq. 2.1.2.4 and Eq. 2.1.2.5 together, we obtain the following Eq. 2.1.2.6 for symmetrical (z : z) electrolyte

$$\frac{d\psi}{dx} = -\left(\frac{8k_B T c_0}{\varepsilon_r \varepsilon_0}\right)^{1/2} \sinh\left(\frac{ze\psi}{2k_B T}\right) \qquad (2.1.2.6)$$

The characteristic distance for the diffuse layer thickness is given as

$$\kappa = \left(\frac{2c_0 z^2 e^2}{\varepsilon_r \varepsilon_0 k_B T}\right)^{1/2} \qquad (2.1.2.7)$$

Where κ is given in m^{-1}.

The charge density of the diffuse layer is given as

$$\sigma_M = \varepsilon_r \varepsilon_0 \left(\frac{d\psi}{dx}\right)_{x=0} = \left(8k_B T \varepsilon_r \varepsilon_0 c_0\right)^{1/2} \sinh\left(\frac{ze\psi_0}{2k_B T}\right) \qquad (2.1.2.8)$$

By differentiating, the differential capacitance is obtained as

$$C_{GC} = \varepsilon_r \varepsilon_0 \kappa \cosh\left(\frac{ze\psi_0}{2k_B T}\right) \qquad (2.1.2.9)$$

From GC model we can expect that from Eq. 2.1.2.9, capacitance shows dependence on potential and also on thickness of the diffuse layer depends on electrolyte concentration (Eq. 2.1.2.7).

In GC model ions are considered as point charges that can approach the surface arbitrarily closely. Therefore at high polarization, the effective separation distance between electrode and solution phase decreases continuously towards zero. This view is not realistic. The ions have a finite size and cannot approach the electrode surface any closer than the ionic radius. However, the GC model leads to an overestimation of the EDL capacitance. The capacitance of two separated sheets of charges increases inversely with their distance of separation, hence a very high capacitance value would arise in the case of point charge ions close to the electrode surface. For low concentration electrolytes, this theory has been successful [11] in predicting ionic profiles close to planar surfaces. But with more concentrated

electrolytes, the charge in solution becomes more compressed and the whole system begins to resemble the Helmholtz model.

2.1.3 Gouy-Chapman-Stern (GCS) Double Layer Model

Stern [12] simply developed the double layer model by suggesting a more realistic way of describing the physical situation at the electrode/electrolyte interface. He combined the Helmholtz model and the Gouy-Chapman model together by introducing a charge free layer nearer to the electrode surface along with diffuse layer in which ions are stored, see Figure 3 c. This charge free layer named as the inner, compact, Helmholtz, or stern layer. He took into account the fact that ions have finite size, and consequently the closest approach of OHP to the electrode shall vary with the ionic radius. Thus the capacitance of the electrical double layer is given as

$$\frac{1}{C_S} = \frac{1}{C_H} + \frac{1}{C_{GC}} \qquad (2.1.3.1)$$

To describe the transport of ions into the EDLs we assume the local equilibrium in the EDL layer of few nanometres in thickness. By using GCS theory the ion concentration at a distance x from the OHP $c_i(x)$ can be related to the ion concentration in the bulk solution, c_i^0, given by

$$c_i(x) = c_i^0 \exp\left(-z_j \psi_d(x)\right) \qquad (2.1.3.2)$$

Where $\psi_d(x)$ is dimensionless potential at a distance x in the diffuse layer defined as the dimensional potential ψ divided by the thermal voltage V_T=RT/F~25.7 mV and z_i = +1 for the cation and z_i = -1 for the anion for NaCl. Therefore, the excess concentration of ion i at any distance from the OHP is

$$c_i - c_i^0 = c_i^0\left(\exp\left(-z_i \psi_d(x)\right) - 1\right) \qquad (2.1.3.3)$$

By integrating Eq. 2.1.3.3, for 1:1 salt, the general equations for excess surface ion adsorption are

$$\begin{aligned}\Gamma_+ &= 2\lambda_d c_0\left(\exp(-\frac{1}{2}\Delta\psi_d)-1\right)\\ \Gamma_- &= 2\lambda_d c_0\left(\exp(\frac{1}{2}\Delta\psi_d)-1\right)\end{aligned} \qquad (2.1.3.5)$$

Where Γ_+ is the excess surface cation adsorption, Γ_- is the excess surface anion adsorption and $\Delta\psi_d$ is the nondimensionless electrical potential difference over the diffuse part of the double layer. Thus the total removed amount of salt upon applying a cell voltage salt adsorption per surface area Γ_{salt} is the sum of the two given by

$$\Gamma_{salt} = \Gamma_+ + \Gamma_- = 2\lambda_d c_0\left(\exp(-\frac{\Delta\psi_d}{2})+\exp(\frac{\Delta\psi_d}{2})-2\right) = 4\lambda_d c_0\left(\cosh\frac{\Delta\psi_d}{2}-1\right) \qquad (2.1.3.6)$$

The surface charge density per unit area of the electrode, σ, in mol/m^2 is given by the difference of Γ_+ and Γ_-

$$\sigma = \Gamma_+ - \Gamma_- = 2\lambda_d c_0\left(\exp(-\frac{\Delta\psi_d}{2})-\exp(\frac{\Delta\psi_d}{2})\right) = 4\lambda_d c_0\left(\sinh\frac{\Delta\psi_d}{2}\right) \qquad (2.1.3.7)$$

Where λ_d is the Debye length, given by $\lambda_d=1/\kappa$, with the inverse Debye length, κ, is given by

$$\kappa^2 = \frac{2F^2 c_0}{\varepsilon_r \varepsilon_0 RT} = 8\pi\lambda_B c_0 N_{av} \qquad (2.1.3.8)$$

Where ε_r the relative permittivity of the medium, ε0 is is the permittivity of the free space, R is the universal gas constant, λ_B is the Bjerrum length [6] and N_{av} is the Avogadro's number.

Finally the charge efficiency of the electrodes for 1:1 salt type can be calculated by taking the ratio of total surface adsorption to surface charge

$$\Lambda = \frac{\Gamma_{salt}}{\sigma} = \frac{\cosh\frac{\Delta\psi_d}{2} - 1}{\sinh\frac{\Delta\psi_d}{2}} = \tanh\frac{\Delta\psi_d}{4} \qquad (2.1.3.9)$$

Now the differential charge efficiency λ, can be derived as follows

$$\lambda = \frac{\Phi_{salt}}{J} = \frac{d\Gamma_{salt}}{d\sigma} = \tanh\frac{\Delta\psi_d}{2} \qquad (2.1.3.10)$$

Where $\Phi_{salt} = \frac{d\Gamma_{salt}}{dt}$ and $J = \frac{d\sigma}{dt}$ (2.1.3.11)

The GCS model assumes a diffuse layer which has a extension to free solution region with thickness of several times the Debye length which is ~3 nm at 10 mM salt concentration and micro pores [6] in porous electrodes are small (< 2 nm), which results in overlapping of the double layers. However, applying this theory to experimental data using standard electrodes made of porous activated carbons, Biesheuvel and co group [6] found [4] that at high cell voltages this theory predicts co-ion expulsions from the EDL that are beyond the amount of co-ions initially present in an electrode. This anomaly is due to the fact that GCS-theory cannot be applied to micro pores where the Debye length is of the order of, or larger than, the pore size. This problem is resolved when mD-model is applied to electrosorption of ions. Because of this overlapping effect GCS model do not take consideration of concentration in micropores of the electrodes and leading to a lower electrosorption capacity. This led us to use modified donnan model to describe the electrical double structure in micropores.

2.1.4 modified Donnan (mD) Double Layer Model

As discussed in the literature [6], mD model is used to describe the ion storage and adsorption in micropores of the porous carbon electrodes. In this approach there are two modifications from GCS model. First is to include stern layer [1], in between pore solution and the carbon matrix, and secondly chemical attraction energy μ_{att} [13] for the ion to go from macroprores into the micropores.

According to mD model concentration of the ions in the micropore related to the macropore salt concentration is given by

$$c_{j,mi} = c_{salt,ma} \exp(-z_j \Delta\Phi_d + \mu_{att}) \quad (2.1.4.1)$$

Where z_j = +1 for cation and z_j = -1 for NaCl, and $\Delta\Phi_d$ is the donnan potential. By adding cation and anion concentration in the micropores gives the total ion density in the micropores

$$c_{ions,mi} = \sum_{j}^{2} c_{j,mi} = 2c_{salt,ma} \exp(\mu_{att}) \cosh(\Delta\Phi_d) \quad (2.1.4.2)$$

The local volumetric ionic charge density (mol/m^3) in the micropores is given by

$$\sigma_{mi} = \sum_{j}^{2} z_j c_{ions,mi} = -2c_{salt,mi} \exp(\mu_{att}) \sinh(\Delta\Phi_d) \quad (2.1.4.3)$$

Now we can define charge efficiency of the EDLs as the total ionic concentration, relative to value at zero charge ($\Delta\Phi_d$=0)

$$\Lambda = \frac{c_{ions,mi} - c^0_{ion,mi}}{\sigma_{mi}} = \tanh\frac{\Delta\Phi_d}{2} \quad (2.1.4.4)$$

According to mD model we can derive differential charge efficiency λ

$$\lambda = \frac{\Phi_{salt}}{J} = \frac{dc_{ion,mi}}{d\sigma_{mi}} = \tanh\Delta\Phi_d \quad (2.1.4.5)$$

Where $\Phi_{salt} = \frac{dc_{ion,mi}}{dt}$ and $J = \frac{d\sigma_{mi}}{dt}$

3 Modelling Scheme and Analysis

Equations governing the physics that are used in the analysis are described below along with the boundary conditions and the parameters used in the analysis. The simulations are performed for both and batch-mode experiments and single-pass mode experiments by using various operational parameters.

3.1 Gouy-Chapman-Stern Layer Model

To model electrosorption phenomena in a flow cell we use the Gouy-Chapman-Stern model. To describe electrosorption process according to GCS model we make several assumptions: 1. we consider a planar electrode surface, 2. we neglect ion volume constraints [14], 3. We assume that the two electrodes are perfectly non-Faradic [15, 16]; i.e., no current is assumed to flow via electrochemical reactions from the electrodes into solution, or vice versa, 4. we neglect the possibility of direct chemical ion adsorption or desorption on the electrode surface.

To describe the ion transport from bulk solution to the interface, we use an approximate approach based on the concept of a mass-transfer layer [17] (diffusion layer, or convective-diffusion layer), present in front of the electrodes.

We describe electrosorption process by assuming a flow cell [Fig. 1], being the space in between the electrodes through which electrolyte solution passes. First we set up salt mass balance in which the accumulation of salt is determined by migration of ions into the electrode, and by convective flow through the flow cell, given by

$$V\frac{dc}{dt} = Q(c_0 - c) - N_{salt} \tag{3.1.1}$$

Where V is the volume of the flow cell, Q the volumetric solution flow rate, c the salt concentration, c_0 the influent salt concentration and N_{salt} the rate by which ions are removed from solution and adsorbed at the electrodes. Our approach is analogous to ohm's law for charge transport in an electric field. In this approach we neglect diffusion (concentration gradients) effect of ions and only consider the effect of the electric filed (migration) as the driving force for the ions. Therefore the net flux of the ions into the electrode; J (mol/m^2s) is given by

$$J = \kappa c \Delta\psi_{mtl} \tag{3.1.2}$$

Here κ (m/s) is mass-transfer coefficient and $\Delta\psi_{mtl}$ the nondimensional electric potential difference across the mass-transfer layer. When compared to ohm's law, k.c in Eq. 3.1.2 plays the role of electrical conductance (one over an electrical resistance). We spilt this factor in a concentration independent term k and the ion concentration c. This shows that resistance and ion concentration are inversely proportional to each other i.e. resistance increases with the decrease in the ion concentration.

We can define the salt removal rate N_{salt} which required in Eq. 3.1.1 as

$$N_{salt} = AJ\lambda \tag{3.1.3}$$

Where A is the area of the electrode (in our case A is same for both electrodes) and λ is the differential charge efficiency derived in the section 2.1.4 and given by

$$\lambda = \tanh\frac{\Delta\psi_d}{2} \tag{3.1.4}$$

Applied voltage V_{cell} is homogeneously distributed between the electrodes in the flow cell which is related to $\Delta\psi_{mtl}$, $\Delta\psi_{st}$, and $\Delta\psi_d$ as follows

$$\frac{1}{2}\frac{V_{cell}}{V_T} = \Delta\psi_{mtl} + \Delta\psi_d + \Delta\psi_{st} \tag{3.1.5}$$

Where $\Delta\psi_{st}$ is the voltage difference over the stern layer and relates directly to σ according to Gauss' law

$$C_{st}\Delta\psi_{st}V_T = \sigma F \tag{3.1.6}$$

Where C_{st} (F/m^2) is the stern layer capacity and F (C/mol) the faraday's number and V_T is the thermal voltage. In the GCS model the surface charge density, σ, is given by

$$\sigma = 4\lambda_d c_0\left(\sinh\frac{\Delta\psi_d}{2}\right) \tag{3.1.7}$$

Finally we must relate the charge density on the electrode surface σ to the charge transport rate, J, through the mass transfer layer according to

$$\frac{d\sigma}{dt} = \frac{A}{a} J \tag{3.1.8}$$

Where a is the effective electrode area (m^2) available for the ion adsorption.

3.1.1 Model Parameters

We simulate the model for various parameters as below.

Parameter	Value	Unit	Description
λ_B	0.72	nm	Bjerrum length
K	sqrt(8*π* λ_B*c_0*N_{av})	1/m	Inverse Debye length
V_T	25.7	mV	Thermal voltage
C_{st}	0.0352	F/m^2	Stern layer capacitance
a	14840	m^2	Effective area available for adsorption
k	0.438	μm/s	Mass-transfer coefficient

Table 1.Parameters setting for GCS model

3.1.2 Analysis

We simulate charge adsorption in a 2D flow cell by using a finite element method based simulation package (COMSOL multiphysics). The problem is modelled in a 2D rectangular flow cell, having a length of 7.5 cm (flow direction) and a width of 1.3mm. The potential difference is applied to longer sides of the rectangle (electrodes). In GCS model C_{st}, a, and k are the fitting parameters. First, we obtain parameter estimates for C_{st}, a, and k by solving the set of Eqs. (3.1.1)- (3.1.8) presented in the section 3.1 at equilibrium state i.e. batch mode experiments. Then we use the same parameter values obtained from the equilibrium to analyze the electrosorption process in single-pass experiments by solving same set of Eqs. (3.1.1)- (3.1.8). The model is solved using graduated mesh with finer mesh near the electrodes and by applying appropriate boundary conditions. To solve this model at equilibrium, total volume of the flow cell V, and electrode geometrical area A are obtained from the experimental geometry. From fitting of the GCS model to

equilibrium experimental data we obtain parameter estimates for C_{st}, a and k. We presented our simulation results for both batch-mode experiments and single pass experiments in results and discussion section.

3.2 Modified Donnan (mD)-Model

In this section we use mD model theory to analyze the electrosorption process. Similarly as we did in GCS model first we assume a flow cell [Fig.1]. We consider only the migration of ions into the electrode as the driving force and velocity of the flow can be given by convective force.

In our approach we assumed that macropore concentration is constant across the electrode. To describe the current voltage relation as we did in GCS, we will not assume a constant resistance but include how the resistance increases when the salt concentration goes down (analogous ohm's law). We assume that at each time the salt concentration within the electrode macropores is the same as in the flow cell.

Therefore, the net flux of the ions into the electrode, J, is given by

$$J = \kappa c \Delta\psi_{mtl} \tag{3.2.1}$$

Here c is the salt concentration in the flow cell, κ (m/s) is mass-transfer coefficient and $\Delta\psi_{mtl}$ the nondimensional electric potential difference across the mass-transfer layer. We can define the salt removal rate N_{salt} as

$$N_{salt} = AJ\lambda \tag{3.2.2}$$

Where A is the area of the electrode and λ is the differential charge efficiency derived in the section 2.1.5 and given by

$$\lambda = \tanh\Delta\psi_{d} \tag{3.2.3}$$

Applied voltage V_{cell} is homogeneously distributed between the electrodes in the flow cell which is related to $\Delta\psi_{mtl}$, $\Delta\psi_{st}$, and $\Delta\psi_{d}$ as follows

$$\frac{V_{cell}}{V_T} = \left(\Delta\Phi_{st} + \Delta\Phi_{d}\right)_{anode} + \Delta\Delta_{mtl} - \left(\Delta\Phi_{st} + \Delta\Phi_{d}\right)_{cathode} = \Delta\psi_{mtl} + 2\left|\Delta\Phi_{st} + \Delta\Phi_{d}\right| \tag{3.2.4}$$

Where $\Delta\psi_{st}$ is the voltage difference over the stern layer and relates directly to σ_{mi} according to Gauss' law

$$C_{st}\Delta\psi_{st}V_T = \sigma_{mi}F \tag{3.2.5}$$

Where C_{st} (F/m^3) is the volumetric stern layer capacity and F (C/mol) the faraday's number and V_T is the thermal voltage.

In mD model we will not use constant stern layer capacitance to fit the data, but use a function where C_{st} increases with increasing charge [18, 19, 20], which we describe empirically by using $C_{st} = C_{st0} + \alpha\sigma_{mi}^2$. Here α is a parameter which describes the non linear part of the stern layer capacitance. In mD model the volumetric charge density, σ_{mi}, is given by

$$\sigma_{mi} = -2c_{salt,mi}\exp(\mu_{att})\sinh(\Delta\Phi_d) \tag{3.2.6}$$

Finally, we set up a balance starting that the total number of moles of salt molecules in the system is conserved,

$$V_{tot}c_0 + V_{mi}c_{ions,mi,0} = V_{tot}c_{cell} + V_{mi}c_{ions,mi} = V_{mi}\gamma \tag{3.2.7}$$

Where V_{mi} is the micropore volume and γ the total amount of salt molecule in the system. From mD theory, at any time, concentration in the micropores of the electrodes is given by

$$c_{ions,mi} = \sqrt{\sigma_{mi}^2 + (2c\exp(\mu_{att}))^2} \tag{3.2.8}$$

Thus the salt concentration in the flow cell from Eq. 3.2.8 is given by

$$c = \frac{\sqrt{b^2 - 4\beta(\sigma_{mi}^2 - \gamma^2)} - b}{2\beta} \tag{3.2.9}$$

$$\text{Where } \beta = (2\exp(\mu_{att}))^2 - \left(\frac{V_{tot}}{V_{mi}}\right)^2 \text{ and } b = 2\gamma\frac{V_{tot}}{V_{mi}} \quad (3.2.10)$$

Finally, the water leaving the flow cell is mixed up with total volume at the outlet is given by

$$V_{tot}\frac{dc_{eff}}{dt} = Q(c_0 - c_{eff}) - N_{salt} \quad (3.2.11)$$

Where V_{tot} is the volume of the flow cell, Q the volumetric solution flow rate, c_{eff} the effluent salt concentration, c_0 the influent salt concentration and N_{salt} the rate by which ions are removed from solution and adsorbed at the electrodes along with we must relate micropore ion density σ_{mi} to the flux of the ions into the electrode according to,

$$V_{mi}\frac{d\sigma_{mi}}{dt} = JA \quad (3.2.12)$$

3.2.1 Model Parameters

We simulate the model for various parameters as below.

Parameter	Value	Unit	Description
$C_{st,0}$	30	MF/m^3	Stern layer capacitance
μ_{att}	1.5		Attraction force
k	0.18	μm/s	Mass-transfer coefficient
α	1.3	Fm^3/mol^2	parameter to describe non-linear part of Stern capacity

Table 2.Parameters setting for mD model

3.2.2 Analysis

We simulate charge adsorption in a 2D flow cell by using a finite element method based simulation package (COMSOL multiphysics). The problem is modelled in a 2D rectangular flow cell, having a length of 7.5 cm (flow direction) and a width of 1.3mm. The potential difference is applied to longer sides of the rectangle

(electrodes). In mD model $C_{st,0}$, α, μ_{att} and k are the fitting parameters. First, we obtain parameter estimates for $C_{st,0}$, α, μ_{att} and k by solving the set of Eqs.(3.2.1)-(3.2.12) presented in the section 3.2 at equilibrium state. Then we use the same parameter values obtained from the equilibrium to analyze the single-pass experiments by solving same set of Eqs.(3.2.1)-(3.2.12). The model is solved using graduated mesh with finer mesh near the electrodes and by applying appropriate boundary conditions. To solve this model at equilibrium, total volume of the flow cell V_{tot}, V_{mi} and electrode geometrical area A are obtained from the experimental geometry. From fitting of the mD model to equilibrium experimental data we obtain parameter estimates for $C_{st,0}$, α, μ_{att} and k. We presented our simulation results for both batch-mode experiments and single pass experiments in results and discussion section.

List of constants used for the analysis of both GCS model and mD model are presented in the appendix A.

4 Results and Discussion

4.1 Simulation Results for GCS Model

In Figure 4, we present both experimental and theoretical result for the effluent salt concentration in a flow cell, as a function of time. Results are presented for both batch mode experiments (Fig. 4 a) and single pass mode experiments (Fig. 4 b).

In the batch mode, experiments were conducted in a different flow cell (not shown here), but with dimensions having a length of 7.5 cm (flow direction) and a width of 1.3mm, with a storage vessel volume of 1 litre, area of the each electrode being 180 cm^2, 1.2 V applied potential, with an input concentration of 599 ppm NaCl, the results of which are shown on Figure 4 a (experimental data). The theoretical data is generated using the GCS model, and the above conditions, and fitted to the experimental data. Basis this, we obtain the fitting parameters C_{st}=0.0352 [F/m^2], a=14840[m^2] and k=0.438 [μm/s], which are further used to generate the theoretical data for single pass experiments.

Single pass experiments were conducted for a similar flow cell (not shown here), with a flow cell volume of 22.5 ml, flow rate of 10 ml/min, with an input concentration of 559 ppm NaCl, an applied potential of 1.2 V was applied for 360s, followed by 10 s of short circuit, followed by 10 s of -1.2 V, followed by 560 s of 0V, repeated 5 times (Fig. 5), the results of which are shown on Figure 4 b (experimental data). The theoretical data for single pass experiments were generated for the above conditions, using fitting parameters from the batch mode experiments and is presented in Figure 4 b (theoretical data).

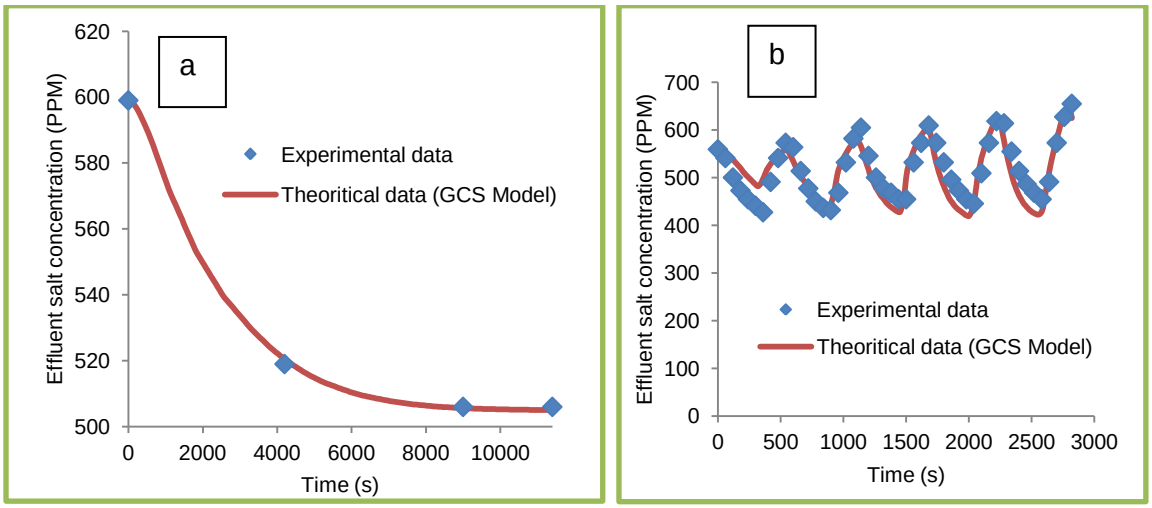

Fig. 4: Effluent salt concentration in a flow cell (GCS Model), (a) Experimental data and Theoretical data for the batch-mode experiments, (b) Experimental data and Theoretical data for the single-pass experiments.

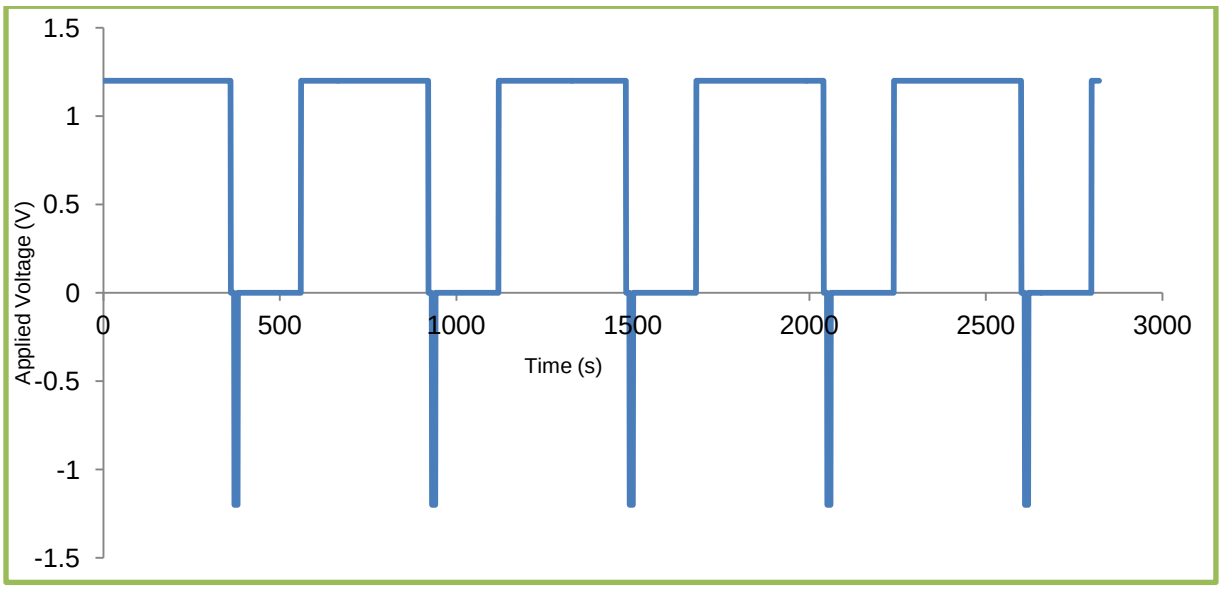

Fig. 5: Step voltages for continuous 5 cycles in single pass experiments. At time zero V_{cell}=1.2 V is applied across each pair of electrodes, which is reduced to zero (short-circuiting the system) at t=360 s, after which V_{cell}=-1.2 V is applied across the electrodes at t=370 s, a voltage which is reduced to zero again at t=380 s.

4.2 Simulation Results for mD Model

Simulations under the same conditions of experimentation, but using the mD model were repeated. The micro pore volume used was V_{mi}=16.5 [ml]. In Figure 6 a, we present both experimental and theoretical result for the effluent salt concentration in a flow cell performed in the batch mode. Based on the fitting, we obtained the fitting parameters $C_{st,0}$=30[MF/m^3], μ_{att}=1.5, α=1.3, and k=0.18 [um/s]. By using these fitting parameters, theoretical data was also generated for the single pass experiments (Fig. 6 b).

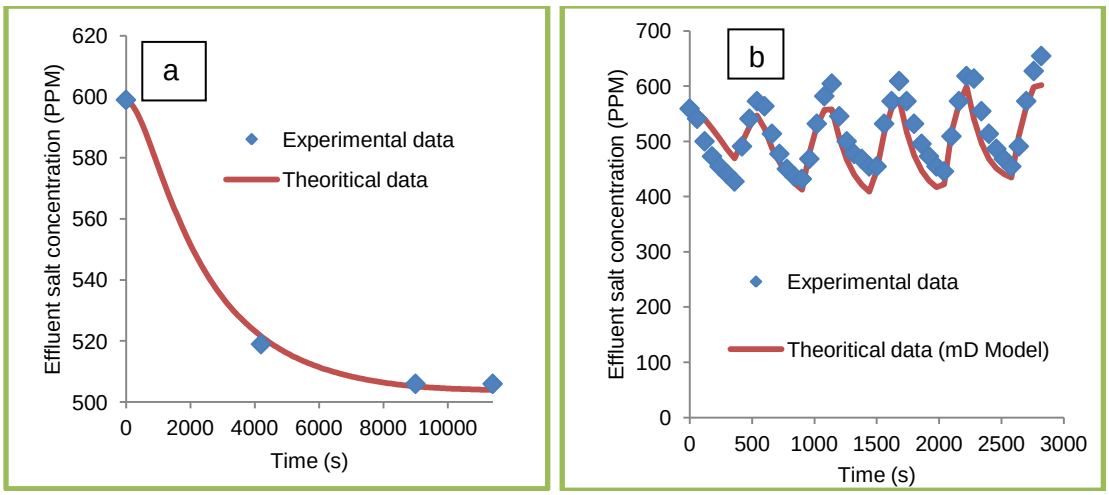

Fig. 6: Effluent salt concentration in a flow cell (mD Model), (a) Experimental data and Theoretical data for the batch-mode experiments, (b) Experimental data and Theoretical data for the single-pass experiments.

The theoretical data and its agreement with experimental data are presented in Figure 4 b (GCS Model) and Figure 6 b (mD Model), and summarised together in Figure 7 for single pass experiments.

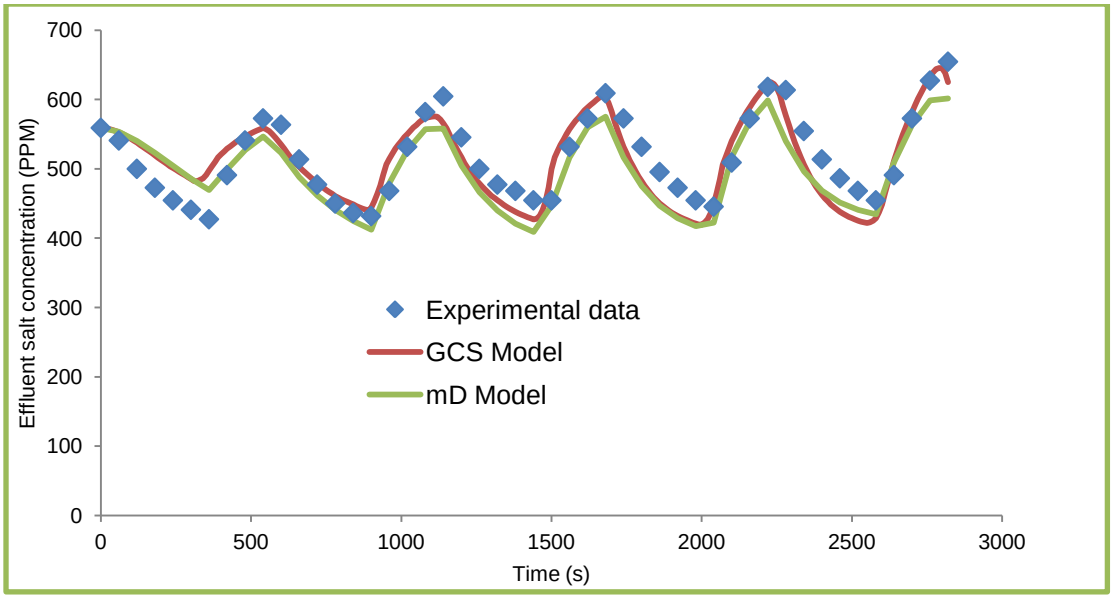

Fig. 7: Comparison between GCS model and mD model with Experimental data

The predictions of the theoretical models for single pass mode experiments shows good agreement to the experimental results with similar magnitudes and profiles for the effluent salt concentration, confirming a good understanding of the electrosorption process and the mechanism therein. It is further seen that the mD model is able to more faithfully reproduce the observed experimental data. This is likely due to a better description of the double layer and its effect due to double layer overlap as expected in the micro pores of the adsorbing surface.

5 Conclusions and Next Steps

In this study, we have been able to confirm the applicability of the GCS and mD model to describe and predict the cyclic electrosorption and desorption process in a continuous flow cell, akin to a CDI system. A 2D model with an ability to input various conditions and derive the salt concentration variation from the flow cell has been implemented in COMSOL. It has also been shown, but not discussed here, that trend relating to effluent concentration dependent on flow rate (Fig. 8) and applied voltage can be simulated, though not so accurately yet. We calculated the salt removal from the second adsorption cycle; see Figure 4 b and Figure 6 b, because it is more accurate to experimental data. The percentage of salt removal is a function of influent flow rate (Fig. 8) can be representatively shown. Salt removal

increases with increasing applied potential because of enhanced adsorption and decreases with increasing flow rate, due to lower residence time in the flow cell

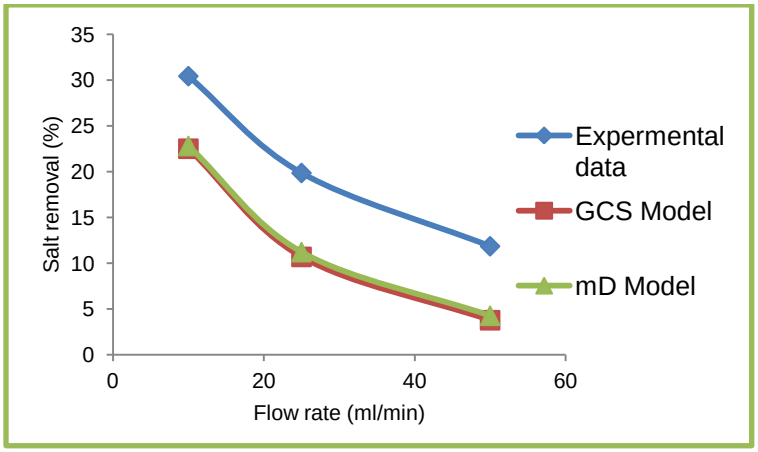

Fig. 8: Effect of flow rate on salt removal

In furthering this work, we propose to further study the dependence of different operational parameters like flow rate and applied potential on electrosorption process without the need to run multiple experiments in batch mode to derive the fitting parameters in each case.

References

[1] Zhao, R.; Van Soestbergen, M.; Rijnaarts, H. H. M.; Van Der Wal, A.; Bazant, M. Z.; Biesheuvel, P. M. Time-Dependent Ion Selectivity in Capacitive Charging of Porous Electrodes. *Journal of colloid and interface science* **2012,** *384,* 38-44.

[2] Johnson, A. M.; Newman, J. Desalting by Means of Porous Carbon Electrodes. *Journal of the Electrochemical Society* **1971,** *118,* 510-517.

[3] Newman, J. S.; Tobias, C. W. Theoretical Analysis of Current Distribution in Porous Electrodes. *Journal of the Electrochemical Society* **1962,** *109,* 1183-1191.

[4] Zhao, R.; Biesheuvel, P. M.; Miedema, H.; Bruning, H.; Van Der Wal, A. Charge Efficiency: a Functional Tool to Probe the Double-Layer Structure Inside of Porous Electrodes and Application in the Modeling of Capacitive Deionization. *The Journal of Physical Chemistry Letters* **2009,** *1,* 205-210.

[5] Biesheuvel, P. M.; Van Limpt, B.; Van Der Wal, A. Dynamic Adsorption/Desorption Process Model for Capacitive Deionization. *The Journal of Physical Chemistry C* **2009,** *113,* 5636-5640.

[6] Porada, S.; Zhao, R.; Van Der Wal, A.; Presser, V.; Biesheuvel, P. M. Review on the Science and Technology of Water Desalination by Capacitive Deionization. *Progress in Materials Science* **2013,** *58,* 1388-1442.

[7] Helmholtz, H. v. Studien ++Ber Electrische Grenzschichten. *Annalen der Physik* **1879,** *243,* 337-382.

[8] Zhang, L. L.; Zhao, X. S. Carbon-Based Materials As Supercapacitor Electrodes. *Chemical Society Reviews* **2009,** *38,* 2520-2531.

[9] Chapman, D. L. LI. A Contribution to the Theory of Electrocapillarity. *The London, Edinburgh, and Dublin Philosophical Magazine and Journal of Science* **1913,** *25,* 475-481.

[10] Gouy, M. Sur La Constitution De La Charge Electrique a La Surface D'Un Electrolyte. *J. Phys. Theor. Appl.* **1910,** *9,* 457-468.

[11] Gongadze, E.; Petersen, S.; Beck, U.; van Rienen, U. Classical Models of the Interface between an Electrode and an Electrolyte. COMSOL Conference , 14-16. 2009.
Ref Type: Conference Proceeding

[12] Stern, O. Theory of the Electrical Double Layer.(In German.). *Electrochemistry* **1924,** *30,* 508-516.

[13] Zhao, R. *Theory and Operation of Capacitive Deionization Systems*; Wageningen University: 2013.

[14] Biesheuvel, P. M. Thermodynamic Cycle Analysis for Capacitive Deionization. *Journal of colloid and interface science* **2009,** *332,* 258-264.

[15] Biesheuvel, P. M.; Fu, Y.; Bazant, M. Z. Diffuse Charge and Faradaic Reactions in Porous Electrodes. *Physical Review E* **2011,** *83,* 061507.

[16] Biesheuvel, P. M.; Bazant, M. Z. Nonlinear Dynamics of Capacitive Charging and Desalination by Porous Electrodes. *Physical Review E* **2010,** *81,* 031502.

[17] Perez, C. A. R.; Demirer, O. N.; Clifton, R. L.; Naylor, R. M.; Hidrovo, C. H. Macro Analysis of the Electro-Adsorption Process in Low Concentration Nacl Solutions for Water Desalination Applications. *Journal of the Electrochemical Society* **2013,** *160,* E13-E21.

[18] Li, H.; Zou, L. Ion-Exchange Membrane Capacitive Deionization: a New Strategy for Brackish Water Desalination. *Desalination* **2011,** *275,* 62-66.

[19] Grahame, D. C. The Electrical Double Layer and the Theory of Electrocapillarity. *Chemical Reviews* **1947,** *41,* 441-501.

[20] Bazant, M. Z.; Chu, K. T.; Bayly, B. J. Current-Voltage Relations for Electrochemical Thin Films. *SIAM journal on applied mathematics* **2005,** *65,* 1463-1484.

Appendices

Appendix A: List of constants used for the analysis of GCS model and mD model.

We use various constants in the analysis for GCS model and mD model as below.

Constant	Value	Unit	Description
F	96485	C/mol	Faraday constant
N_{av}	6.023e23	1/mol	Avogadro number
ε_r	78.3		Relative permittivity of water
ε_0	8.854e-12	F/m	Permittivity of the free space
R	8.314	J/(mol*K)	Universal gas constant
T	293.15	K	Absolute temperature
π	3.14		Constant Pi value
k_B	1.38e-23	J/K	Boltzmann constant
e	1.602e-19	C	Elementary charge

Table 3: List of constants used for the analysis of GCS model and mD model

Appendix B: Modelling Approach using PNP equation and Langmuir adsorption

B.1 Introduction

The availability of affordable clean water is one of the key social, economic and technological challenges of the 21st century. Over the years a number of deionization methods have been developed, among which multi-stage flash distillation and reverse osmosis are now the most commonly known and wide spread technologies. Multi-stage flash distillation is a thermal desalination process, but is highly energy intensive. Reverse osmosis is a membrane based separation process which is comparatively less energy intensive, but still requires large pressures to desalinate the water and is highly capital intensive. Due to these limitations, there is still a need for a competitive technology that can operate at low cost and is energy efficient. Capacitive deionization (CDI) is a more recent technology that can possibly meet this requirement. It is currently emerging as the most feasible small-scale and low-energy alternative technology to reverse osmosis for the desalination of brackish water. Capacitive deionization works by the principle of electrosorption. Upon applying a potential difference between two parallel porous carbon electrodes, ions from the medium become immobilized by electrosorption process, that is, cations move into the cathode (the electrode into which negative electrical charge is transferred), while anions move into the anode, thereby leaving the water demonized.

In the current project, it is our ambition to model a CDI process to be able to predict operational parameters and their influence on deionization process. We simulate charge adsorption in a 2D flow cell by using a finite element method based simulation package (COMSOL multiphysics) and study its dependence on applied potential and flow rate that can further help design a CDI system.

B.2 Modelling Approach

The problem is modeled in a 2D rectangular flow cell, see Figure 9. The potential difference is applied to two longer sides of the rectangle (electrodes) and the shorter sides act as inlet and outlet for fluid flow. The problem is analyzed by coupling the incompressible Navier-Stokes equation along with Poisson’s equation to

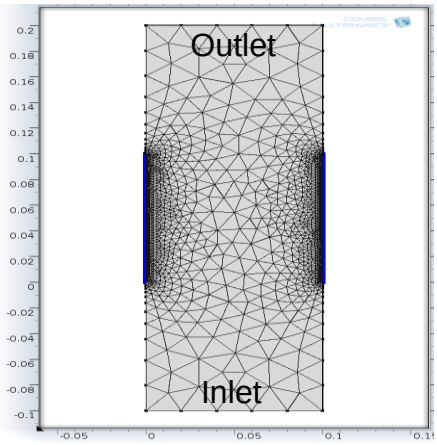

Fig. 9: Geometry & Mesh, rectangular geometry having a length 0.3 mm and a width 0.1 mm and active surface length 0.1 mm

solve for development of flow and electric field in the channel. Alongside, the Nernst-Planck equation provide for the diffusion, migration and convection of the different types of ionic species in the medium. The charge adsorption on the electrodes is determined using a Langmuir adsorption model.

B.3 Results and Discussion

The model is solved using graduated mesh with finer mesh near the electrodes (Fig.9) and by applying appropriate boundary conditions. The simulations are performed for a constant initial concentration for each ion (10 mol/m^3), varying applied potential from 0.5 to 2V and flow rates from 0.41 to 41ml/min. Figure 10 shows the resulting accumulation of counter-ions, accompanied by the depletion of the co-ions, at the electrodes in response to the applied potential. This leads to a reduction in the concentration of ions at the outlet, and consequent deionization of the inlet stream.

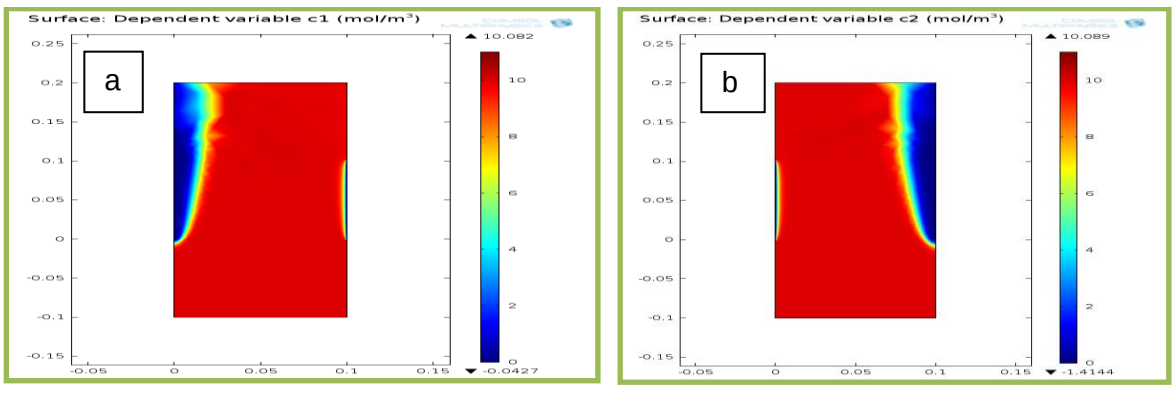

Fig. 10: Ion concentration in the flow channel, (a) Na^+, (b) Cl^-

The ion concentration at the outlet is a function of applied potential (Fig.11 a) and the influent flow rate (Fig. 11 b). Salt removal increases with increasing applied potential because of enhanced charge adsorption and decreases with increasing flow rate, due to lower residence time in the flow cell.

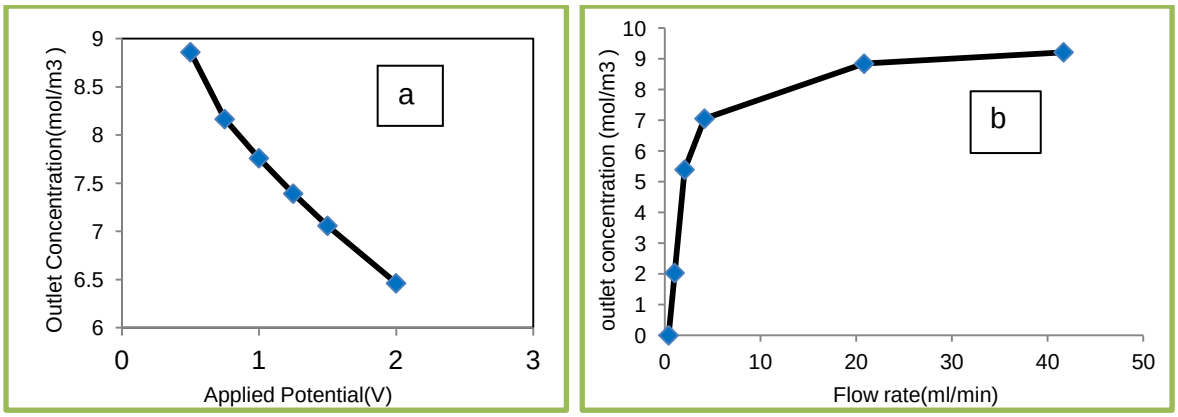

Fig 11: Variation in output concentration as a function of (a) Applied Potential, (b) Flow rate.

B.4 Conclusions

Based on our work this far [1], we concluded that adsorption is proportional to the applied potential and inversely proportional to the flow rate; the salt removal is dependent on charge and diffusivity of the ions. The salt removal predicted by the model is 51% as against 59% obtained experimentally. Further work, as a part of this project, includes the incorporation of porosity of the electrodes, more relevant cell geometries.

References

[1] Venkataraghavan, R.; Tinto Alencherry, J.; Naveen Aerpula. Modeling the adsorption of ions on electrodes in a flow cell. COMSOL Conference, 17-18. **2013**. Ref Type: Conference Proceeding.